J Intell Robot Syst (2018) 90:443–454
https://doi.org/10.1007/s10846-017-0660-0

Output-Feedback Stabilization of the PVTOL Aircraft System Based on an Exact Differentiator

Carlos Aguilar-Ibañez[1] · Miguel S. Suarez-Castanon[2] · Julio Mendoza-Mendoza[1] · Jose de Jesus Rubio[3] · Juan Carlos Martínez-García[4]

Received: 8 August 2016 / Accepted: 26 June 2017 / Published online: 2 November 2017

Abstract An output-feedback control strategy for the regulation of a planar vertical take-off and landing aircraft is presented here. The strategy consists of two controllers that work simultaneously. The first controller stabilizes the vertical variable, and is based on a simple feedback-linearization procedure, in combination with a nonlinear controller (which behaves as a terminal slide mode). The other controller stabilizes the horizontal and angular variables to the desired rest position, and was designed using an energy-control method. The velocities were exactly estimated with a second-order sliding-mode observer. Because this observer computes the velocities in finite time, the control strategy can be designed independently. The effectiveness of the closed-loop system was tested through numerical simulations and compared with other control strategies.

This research was suported by Secretarí a de Investigación y Posgrado del Instituto Politécnico Nacional, under research grants 20160268 and 20161637.

✉ Carlos Aguilar-Ibañez
carlosaguilari@cic.ipn.mx

Miguel S. Suarez-Castanon
sasuarez@prodigy.net.mx

[1] CIC-Instituto Politécnico Nacional, Av. Juan de Dios Bátiz s/n, U.P.A.L.M, Col. San Pedro Zacatenco, A.P. 75476, México, D.F. 07738, Mexico

[2] ESCOM-Instituto Politécnico Nacional, Av. Juan de Dios Bátiz s/n, Mexico, D.F. 07738 Ciudad de México, México

[3] ESIME AZC-Instituto Politécnico Nacional, Av. de Las Granjas 682, 02250 Ciudad de México, México

[4] Control Automático - CINVESTAV del IPN, Av. Instituto Politécnico Nacional 2508, 07360 Ciudad de México, México

Keywords PVTOL aircraft · Sliding mode observer · Energy-based control · Exact differentiator

1 Introduction

Nowadays, unmanned aerial vehicles (**UAV**) have several actual applications. For instance, in security, they perform tasks in reconnaissance, police assistance, and crowd monitoring. In search and rescue, they are used in places where the accessibility is highly complicated and that take a lot of time to explore on foot or using terrestrial vehicles. UAVs improve efficiency and effectiveness in monitoring waterways, civil engineering constructions, oil and gas pipelines, pollution and air sampling, and disaster damage estimation. In the field of communications they can help extend signal coverage. More recently, UAVs have been used to help in the creation of three-dimensional maps and to guide visitors in places like university campuses. Moreover, UAVs have been proposed as a means to provide package delivery to customers who buy products through the internet. However, to be able to apply UAVs in these and other applications, several control mechanism must be designed. Developing these mechanisms is by no means an easy task, among other things because use of these vehicles involves potential physical risk to people. Moreover, deep knowledge of the dynamics and behavior of these vehicles is necessary to be able to propose techniques that allow them to be controlled automatically. Among these UAVs, planar vertical take-off and landing (PVTOL) aircrafts have been studied extensively, because they have several characteristics that make them suitable as a model for developing control techniques that can be used to control actual unmanned flying devices. Among their most important characteristics is that these aircrafts are a simplified version of real flying devices,

like some helicopters and the Harrier Jump Jet [9, 21, 26], though their configuration and behavior allows us to consider them as real aircraft [28, 37, 40, 49]. Traditionally, a PVTOL aircraft consists of two rotors that work independently of each other. These rotors produce a force and a moment over the aircraft. In Fig. 1 shows a representation of a PVTOL aircraft, where we can see that it has three degrees of freedom, the horizontal and vertical positions (x, y), and the angle (θ) that the device makes with respect to the imaginary horizontal line. Another aspect that makes PVTOL aircraft very attractive to develop control techniques is that they belong to a class of systems that cannot be fully controlled - that is, some of its degrees of freedom cannot be directly controlled. Due to the above and the fact that strategies developed for fully controlled systems are useless for this kind of systems, being underactuated, they represent a benchmark for investigating dynamics and control-related issues for UAVs [10, 18, 20, 21, 27].

In the study of PVTOL aircrafts, two branches can be identified: one devoted to developing stabilization control techniques (see, for instance [18, 29, 38, 39, 50]), and the other to proposing solutions to the tracking control problem (see [2, 6, 19, 23, 26, 30, 33, 34, 48]). A full review of the works dealing with these topics is beyond the scope of this study; nevertheless, we mention those we consider more important and relevant to our work. Hauser et al. [23] proposed applying an approximated input-output linearization and neglecting the influence of rolling moment on the lateral force, a nonlinear control strategy for a non-minimum phase system, which accomplished bounded tracking and asymptotic stability. Using a similar approach in conjunction with the back-stepping approach, Sepulcher et al. in [41] derived another approximated solution. The small gain theorem was used by Teel in [43] to solve the regulation control problem and was applied to control some systems, among them a PVTOL system. The trajectory tracking problem for a simplified version of a VSTOL was solved in [31] using a differential flatness approach. In [42], the author used differential parameterization and exploited the PVTOL's flatness property for the regulation of the non-minimum phase outputs. An algorithm developed specifically for PVTOLs was presented in [13]. This algorithm is based on forwarding control and ensures asymptotic stability using a Lyapunov function. Based on that work, comparable strategies with real applications for PVTOLs systems were designed in [14, 27, 37, 49]. Olfati-Saber addressed in [35] the global configuration stabilization for the VTOL aircraft with a strong input coupling using a smooth static-state feedback. In addition, the VTOL system flatness property is used to obtain its corresponding outputs in that work. A different algorithm for the planning of feasible and minimum energy paths was introduced in [6]. Its performance was tested numerically using a one-dimensional system and a PVTOL aircraft. In [1], the authors presented an approach based on the combination of an **IDA-PBC** technique and a reduced-order observer. The regulation problem was solved in [45] using a passivity-based control; the authors showed that the PVTOL dynamics can be expressed as an interconnection of passive systems with a pendulum-like sub-system. Based on linear algebra, an attractive control strategy to solve the trajectory control problem for a PVTOL aircraft was introduced in [17]. In [7] and [46], several control strategies for planar vertical takeoff and landing are presented. These strategies assure global asymptotic stability. In [4] and [24], the authors used the sliding mode method to develop a robust control strategy for the PVTOL. Finally, in [2, 6, 15, 17, 19] , several solutions to control the kind of aircraft we are dealing with here can be found. In [16], a state-feedback controller for a PVTOL model where only partial information of their dynamics was available is proposed. The unknown dynamics are recovered using a finite-time observer with fast convergence time. In [7] and [46], several control strategies for planar vertical takeoff and landing are presented. These strategies assure global asymptotic stability. In [47], the authors proposed an alternative cascade structure for the PVTOL model previously proposed by Olfati-Saber [35]. In [44], a controller based on a Lyapunov function with asymptotic stabilization is introduced; the author used the method presented in [3] to design the controller. In [32], the authors proposed a robust control strategy to stabilize a PVTOL aircraft in the presence of crosswind. The solution is based on robust-control Lyapunov functions and Sontag universal stabilizing feedback. The parameters are tuned in real time through the Riccati equation. In [8], a solution to the path-following problem for PVTOL aircraft, which is applicable to a class of smooth Jordan curves, is presented.

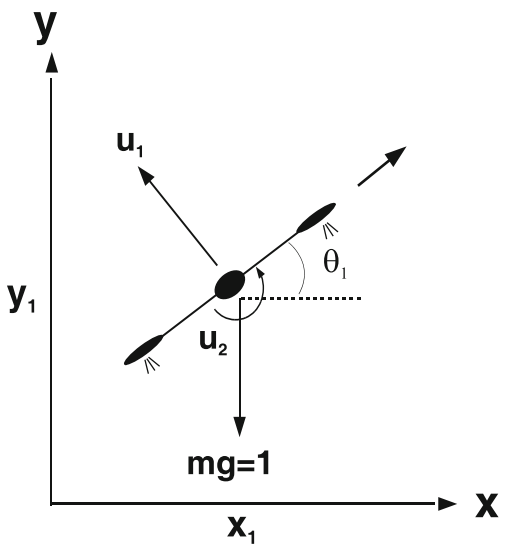

Fig. 1 The PVTOL aircraft (front view)

The obtained controller guarantees that the time average of the roll angle is zero and that the PVTOL aircraft does not perform multiple revolutions about its longitudinal axis. In [19], the authors presented a bounded feedback tracking stabilizer for the PVTOL aircraft where the velocity is not always available. This solution also has uniform global asymptotic stability and uniform local exponential stability of the closed-loop tracking dynamics. In [2], considering actuator limitation constraints, asymptotic-output tracking for the PVTOL aircraft is achieved by using a nonlinear optimal control allocation method presented in [47].

In the present paper, a control strategy for solving the output-feedback regulation problem for the PVTOL system is proposed. To accomplish this, we first design two controllers that work simultaneously, assuming that the whole state is available. We then use a second-order sliding-mode observer for estimating the actual velocities. The controller was designed to be independent from the observer, because it has observation exact finite-time [11]. For designing the controller in charge of stabilizing the vertical position, we use a combination of feedback linearization and a saturation function. This saturation function depends on a nonlinear combination of the vertical variables. The second controller was designed using the basin ideas of the energy-shaping control approach and is devoted to steering the horizontal and angular positions toward to the desired reference.

The remainder of this study is organized as follows. In Section 2, we introduce the theoretical framework used in the forthcoming developments. In Section 3, the proposed solution to the regulation problem of the PVTOL system is developed. The results of the numerical experiments assessing the effectiveness of our control strategy are presented in Section 4, while the concluding remarks are given in Section 5. An Appendix is also included, where the corresponding proofs of some of the required lemmas can be found.

2 Problem Statement

Let us introduce the normalized equations of the PVTOL system, shown in Fig. 1, found in [13]:

$$\begin{aligned} \dot{x}_1 &= x_2; \\ \dot{x}_2 &= -\sin(\theta_1)u_1; \\ \dot{y}_1 &= y_2; \\ \dot{y}_2 &= \cos(\theta_1)u_1 - 1; \\ \dot{\theta}_1 &= \theta_2; \\ \dot{\theta}_2 &= u_2. \end{aligned} \tag{1}$$

where variables x_1 and y_1 are, respectively, the normalized horizontal and vertical positions, and θ_1 is the angle that the PVTOL makes with respect to the imaginary horizontal line; x_2 and y_2 are the normalized horizontal and vertical velocities, respectively, and θ_2 is the angular velocity. The thrust to levitate the PVTOL is u_1, and u_2 is the rolling moment about its corresponding center of mass. The normalized gravity force was fixed at "1". Notice that this system belongs to the class of underactuated systems, because it has three degrees of freedom, (x_1, y_1, θ_1), and two independent controllers, (u_1, u_2).

Control Problem Consider the normalized PVTOL system (1). The goal of this work is to design the smooth controllers, u_1 and u_2, to solve the output-feedback regulation problem for (1), provided that the system positions are available and that the system angle is initialized inside of $I_0 = (-\overline{\theta}, \overline{\theta})$, with $\overline{\theta} < \pi/2$. Formally, we want to propose $u_1(q, \widehat{p})$ and $u_2(q, \widehat{p})$, such that:

$$\lim_{t\to\infty} \|q - \overline{q}\| = 0 \text{ and } \quad \lim_{t\to\infty} \|p\| = 0,$$

where the available position $q = (y_1, x_1, \theta_1)$ is the system output, $p = (y_2, x_2, \theta_2)$ and $\widehat{p}$ are the vector velocity state and it corresponding estimation, respectively, and $\overline{q} = (\overline{y}_1, \overline{x}_1, 0)$ is the desired reference position.

This section is concluded by introducing the following assumptions:

A1: The angle, $\theta(t) \in I_0$, holds for all time.
A2: The position, q, is always available.

Main contributions Compared to previous works, some of which are mentioned in the Introduction, the main contributions of this work are highlighted in the following statements:

- The system has been controlled using many approaches found in the literature. However, we introduce a controller that is able to regulate vertical displacement in a small period of time, avoiding undesirable overshoots in the velocity coordinate. This characteristic is quite convenient when carrying out hovering and landing maneuver tasks.[1] On the other hand, the regulation of the angular and vertical coordinates was achieved using a control scheme based on the shaping energy approach, obtaining a good performance.
- Another advantage of our approach is that it enables a sliding-mode observer that is adequate to solve the output-feedback regulation problem, with a simple stability analysis.

We finish this section by introducing some notation and definitions needed in the forthcoming developments.

[1] In the forthcoming developments we show that manipulating the constant L (see Eq. 2) makes it possible for the system to reach the minimal time response.

Notation and definitions

$\widetilde{w} = w - \overline{w};\ w = \{x, y\},$

where $\overline{w}$ is a fixed constant. The symbol $\delta > 0$ indicates a very small constant; $s_n[*]$ and sgn$[x]$ are used to refer, respectively, to a linear saturation function and the signum function of a real number. That is:

$$s_n[x] = \begin{cases} x : if : |x| \leq n, \\ n : if : x > n, \\ -n : if : x < -n, \end{cases} ;\ \text{sgn}[x]$$
$$= \begin{cases} 1 : if : x > 0, \\ -1 : if : x < 0, \\ \in [-1, 1] : if : x = 0. \end{cases}.$$

3 Control Strategy

First, we introduce our feedback-control strategy, and then we present a super-twisting based observer (**STBO**) adequate to solve the output-feedback regulation problem. The corresponding control strategy consists of designing u_1, which is responsible for maneuvering the vertical position and the vertical velocity of the system, each represented by $y = (y_1, y_2)$. Simultaneously, u_2 is proposed such that it controls the complementary horizontal variables $x = (x_1, x_2)$, and the angular variables $\theta = (\theta_1, \theta_2)$, restricted to $\theta_1 \in I_0$. In order to develop these controllers, we introduce the following lemma:

Lemma 1 *Consider the following second-order system:*

$$\begin{aligned} &\dot{\alpha} = \beta; \\ &\dot{\beta} = -s_r \left[L \left(\widetilde{\alpha} + \tfrac{\beta|\beta|}{2r} \right) \right] = -s_r [L\widetilde{\eta}], \end{aligned} \tag{2}$$

*where $\alpha, \beta \in \mathbb{R}$, and $r > 0$ and $L > 0$. Then, the origin $(\alpha = \overline{\alpha}, \beta = 0)$ of system (2) is **GAS**.*[2] *Evidently, when $L \to \infty$, the second equation of* Eq. 2 *turns out to be $\dot{\beta} = -rsgn[\widetilde{\eta}]$.*

This system behaves as a robust sliding-mode control, having the characteristic of showing less overshoot, particularly over the y -coordinate. Additionally, it is well known that these configurations present a time-optimal solution [22].

The proof of this lemma is in the Appendix.

Controlling the vertical variables Based on [27], the control action u_1 is proposed as follows:

$$u_1 = \frac{1 - s_r [L\widetilde{y}]}{\cos(\theta_1)}, \tag{3}$$

[2] **GAS** refers to "globally asymptotically stable" and "locally exponentially stable."

where $L > 0, 0 < r < 1$ and

$$\widetilde{y} = \widetilde{y}_1 + y_2 |y_2| / (2r)$$

From the above, the system (1) can be rewritten, as:

$$\begin{aligned} &\dot{\widetilde{x}}_1 = x_2; \\ &\dot{x}_2 = \tan(\theta_1)(s_r [L\widetilde{y}] - 1); \\ &\dot{\widetilde{y}}_1 = y_2; \\ &\dot{y}_2 = -s_r [L\widetilde{y}]; \\ &\dot{\theta}_1 = \theta_2; \\ &\dot{\theta}_2 = u_2, \end{aligned} \tag{4}$$

where $\widetilde{x} = [\widetilde{x}_1, x_2]^T$.

Finally, it should be borne in mind that the third and fourth equations of the system of Eq. 4 satisfy the condition in **Lemma 1**. That is, $\widetilde{y}$ is **GAS**, provided that $\theta_1 \in I_0$. Because $(\widetilde{y}, \dot{y})$ is **GAS**, the effect produced by this function can be neglected (this fact is shown below).

Comment 1 As can be seen, the control strategy gives priority to the regulation of the y -coordinate, having both a minimal time response for L that is sufficiently large, and a small overshot (see Section III of [22]).

Designing of controller u_2 based on the energy control approach Observe that, as long as $I_0 = (-\overline{\theta}, \overline{\theta})$, this model is well-defined. This condition is justified below. The needed candidate Lyapunov function is proposed as:

$$V_T(Z) = \frac{1}{2} z_2^T M z_2 + \frac{\Delta}{m_2} \log(\cos\theta_1) + \frac{k_p}{2} \left(\theta_1 + \frac{m_2}{m_3} \widetilde{x}_1 \right)^2, \tag{5}$$

where $z_1 = [x_1, \theta_1]$, $z_2 = [x_2, \theta_2]$, $k_p, m_1, m_3 > 0$, and $m_2 < 0$, and $M > 0$ is fixed as:

$$M = \begin{bmatrix} m_1 & m_2 \\ m_2 & m_3 \end{bmatrix}$$

with $\Delta = m_1 m_3 - m_2^2 > 0$.

Comment 2 This Lyapunov function was designed using the basin ideas of the IDA-PBC approach [1, 36]. That is, function V was proposed by shaping the potential and kinetic energies, through the solution of two matching conditions.

It should be underscored that $V_T(Z)$ is strictly positive and radially bounded for all $\theta_1 \in (-\pi/2, \pi/2)$, if $m_2 < 0$. It is easy to check whether the time derivative of Eq. 5, around the trajectories of Eq. 4, is given by:

$$\dot{V}_T(Z) = u_2(m_3\theta_2 + m_2 x_2) + (m_3\theta_2 + m_2 x_2)\Phi(\widetilde{x}_1, \theta_1), \tag{6}$$

where:

$$\Phi(z_1) = \frac{1}{m_2 m_3^2}\left(k_p m_2 m_3 \theta_1 + k_p m_2^2 \widetilde{x}_1 - m_1 m_3 \tan\theta_1\right), \tag{7}$$

Hence, after fixing u_2, as:

$$u_2 = -\lambda(m_3\theta_2 + m_2 x_2) - \Phi(\widetilde{x}_1, \theta_1). \tag{8}$$

where $\lambda > 0$, it is easy to see that Eq. 6 becomes:

$$\dot{V}_T(Z) = -\lambda(m_3\theta_2 + m_2 x_2)^2. \tag{9}$$

To avoid the singular points $\pm\overline{\theta}$, the following set of admissible solutions for the system (4) should be introduced:

$$A = \{Z = (x_1, \dot{x}_1 = x_2, \theta_1, \dot{\theta}_1 = \theta_2) \in \mathbb{R}^2 \times (-\overline{\theta}, \overline{\theta}) \times \mathbb{R}\}.$$

Evidently, if the system (4) is initialized inside of the following invariant set:

$$\Omega_{\overline{\theta}} = \{Z \subset A : V_T(Z(0)) < \overline{R} = \frac{\Delta}{m_2}\log(\cos\overline{\theta})\}, \tag{10}$$

then we have that $V_T(Z(t)) < \overline{R}$, for all $t \geq 0$. This means that $Z \in \Omega_{\overline{\theta}}$.

Comment 3 The set $\Omega_{\overline{\theta}}$ has the property that all the solutions of the closed-loop system (defined by Eqs. 8 and 4) that start in $\Omega_{\overline{\theta}}$ remain in $\Omega_{\overline{\theta}}$ forever. That is, $\Omega_{\overline{\theta}}$ is an invariant set for the closed-loop system. In addition, this set is needed to apply LaSalle's invariance theorem [25] to prove convergence to the origin of Z. It is important to note that the proposed solution gives a higher priority to the convergence of the y-coordinate. Additionally, to solve the regulation of variables (x, θ) a reduced-order energy method was used. This solution differs from the one presented in [1], which applies the IDA-PBC approach for the whole system.

Convergence at the origin of variables $(\boldsymbol{\theta}, \boldsymbol{z})$ Since the proposed function, V_T, is strictly positive and definite in $\Omega_{\overline{\theta}}$ and $\dot{V}_T$ is a semi-definite negative function, stability of the equilibrium point in the Lyapunovian sense is concluded. To complete the proof, it is necessary to use LaSalle's invariance theorem. To do so, it is necessary to compute the largest invariant set M contained in the set S, where S is defined as:

$$S = \left\{Z \in \Omega_{\overline{\theta}} : (m_3\theta_2 + m_2 x_2) = 0\right\}.$$

After some tedious considerations, it can be concluded that M is constituted by the single point $M = \{Z = 0\}$. According to LaSalle's theorem, all the trajectories of the closed-loop system that start inside the set $\Omega_{\overline{\theta}}$ asymptotically converge toward to the largest invariant set contained in S, which is the equilibrium point $Z = 0$.

The previous discussion is summarized in the following proposition. For this goal, the set of admissible control gains is defined as:

$$K = \{\kappa = (0 < r < 1, L > 1, \lambda > 0, m_1 > 0, m_2 < 0 \\ \Delta = m_1 m_3 - m_2^2 > 0, k_p > 0)\} \in \mathbb{R}^7. \tag{11}$$

Proposition 1 *Consider the nonlinear system* (1)*, in closed loop with* (u_1, u_2)*, where:*

$$\begin{aligned} u_1 &= \frac{1 - s_r\left[L\left(\widetilde{y}_1 + \frac{y_2|y_2|}{2r}\right)\right]}{\cos(\theta_1)}, \\ u_2 &= -\lambda(m_3\theta_2 + m_2 x_2) - \Phi(\widetilde{x}_1, \theta_1) \end{aligned} \tag{12}$$

and:

$$\Phi(z_1) = \frac{1}{m_2 m_3^2}\left(k_p m_2 m_3 \theta_1 + k_p m_2^2 \widetilde{x}_1 - m_1 m_3 \tan\theta_1\right).$$

Assuming that the control gains $\kappa \in Q$ *are selected according to* Eq. 11*, then the origin of the closed-loop system is locally asymptotically stable, with its corresponding domain of attraction defined by* Eq. 10*.*

Comment 4 Evidently, the set $\Omega_{\overline{\theta}}$ can be enlarged as desired. To do so, the parameters of M can be fixed, such that $\Delta/m_2 << 1$, or the values of $\overline{\theta}$ can be fixed sufficiently close to $\pi/2$.

Numerical simulations In this section we test the robustness of our control strategy and compare its performance with two other well established control techniques. To this end, we designed two numerical experiments. In the first experiment we use the simplified model (1), and consider the presence of small perturbations that act in the acceleration of variable x y y. In the second experiment, we use the more complete model, given below in Eq. 14, and in which the structural parameter ϵ is unknown for the design of the control laws.

First experiment in this experiment we compared our control strategy (**OCL**), defined in Eq. 12, with the control techniques proposed by Fantoni et al. in [14] and by Munoz et al. in [32], respectively referred to as (**FCL**) and (**MCL**). The control task consisted of bringing the PVTOL from the initial rest position $(y_{1_0} = 6.1, x_{1_0} = -0.6, \theta_{1_0} = 0.8)$, to the a final rest position close to the origin. The persistent perturbation, added to the accelerations of variables y and x, was defined as $\omega(t) = 0.08\sin(t)\cos(t)$, for all t. The corresponding control gains were:

$$\begin{matrix} m_1 = 0.85 & m_2 = -0.72 & m_3 = 0.85 \\ r = 0.6 & L = 150 & k_p = 1 \end{matrix}, \tag{13}$$

with $\overline{\theta} = 0.99\pi/2$. The control gains of FCL and MCL were taken from [14] and [32], respectively. The obtained results

are shown in Fig. 2, which shows that OCL behaves as well as MCL does. However, in steady-state, OCL exhibits a better performance than the performance of both FCL and MCL. We must recall that MCL was proposed under a robust control scheme based on Sontag's formula, while OCL and FCL were designed without considering external perturbation.

Second experiment in this simulation we compare our control law OCL with two strategies: the H_∞ (**HIL**) and the slide-mode control (**SMC**). To this end, we consider a more complete model than the system (1), given by:

$$\begin{aligned} \ddot{y}_1 &= \cos(\theta_1)u_1 - 1 + \varepsilon u_2 \cos\theta_1 + \omega_1(t); \\ \ddot{x}_1 &= -\sin(\theta_1)u_1 + \varepsilon u_2 \cos\theta_1 + \omega_2(t); \\ \ddot{\theta}_1 &= u_2 + \omega_3(t), \end{aligned} \tag{14}$$

where ω_i are small external unknown and bounded perturbations, and $\varepsilon < 1$ is a small and unknown coefficient that characterizes the coupling between the rolling moment and the lateral acceleration of the system. The control task consisted of bringing the system from the initial rest position $(y_{1_0} = 1, x_{1_0} = -0.2, \theta_{1_0} = 0.2)$, to the neighborhood of the origin, with $\epsilon = 0.1$, and:

$$\omega_1 = 0.1 * \sin(t);\ \omega_2 = 0.09 * \sin(t) * \cos(t);\ \omega_3 = \frac{0.1*\sin(t)}{\sqrt{t+1}}$$

The SMC was designed based on the work [4], where the control law u_1 and u_2 were tuned using the same control parameters used in that work. The HIC was designed according to the H_∞ procedure summarized by Castaños et al. in [5]. To this end, we used the feedbacks $u_1 = 1 - \overline{K}_1^T y$ and $u_2 = -\overline{K}_2^T Z$, where:

$$\begin{aligned} \overline{K}_1^T &= (2.4004, 5.2594);\ \overline{K}_2^T \\ &= (-0.4423, -1.2154, 1.8435, 2.3314), \end{aligned} \tag{15}$$

and $y = (y_1, \dot{y}_1 = y_2)$ and $Z = (x_1, \dot{x}, \theta_1, \dot{\theta}_1)$. The detailed procedure to obtain the HIC can be found in the Appendix.

The control parameters used in OCL were the same as those used in the first experiment. To have an intuitive idea of the performance of each strategy, we used the following performance index:

$$J(T) = \frac{1}{T}\int_0^T (Z^T(s)Z(s) + y^T(s)y(s))ds; \quad T > 0.$$

The performance of the control actions of each strategy, with their corresponding performance indexes are shown in Fig. 3. According to the performance indexes, our control law outperforms the other two laws. On the other hand, the behaviors of the controllers of SMC exhibit more chattering, with bigger amplitude than the controllers of other two strategies, even when the sign function was smoothed by $sign(x) = x/(|x| + 10^{-4})$. Additionally, we can see that the amplitudes of u_1 and u_2 of OCL are similar to the ones of the HIC. However, it must be mentioned that if we manipulate the penalty function for the HIC procedure, it is possible to obtain a better performance. It is worthy mentioning that we did not show the plot of the states (Y, Z) because they overlap on top of each and are thus hard to distinguish.

4 Output-feedback Stabilization

The state feedback controllers u_1 and u_2, developed in the previous section require measurements of both the positions and velocities of the system. In this section, the STBO, found in [12], was adequate to estimate the non-available velocity vector $p = (y_2, x_2, \theta_2)$, from the knowledge of the measurement of the vector position $q = (x_1, y_1, \theta_1)^T$. Based on **Proposition 1**, the actual controllers, $\widehat{u}_1$ and $\widehat{u}_2$, were defined as:

$$\begin{aligned} \widehat{u}_1(q, \widehat{p}) &= \tfrac{1-\widehat{r}}{\cos(\theta_1)}, \\ \widehat{u}_2(q, \widehat{p}) &= -\lambda(m_3\widehat{\theta}_2 + m_2\widehat{x}_2) - \Phi(\widetilde{x}_1, \theta_1), \end{aligned} \tag{16}$$

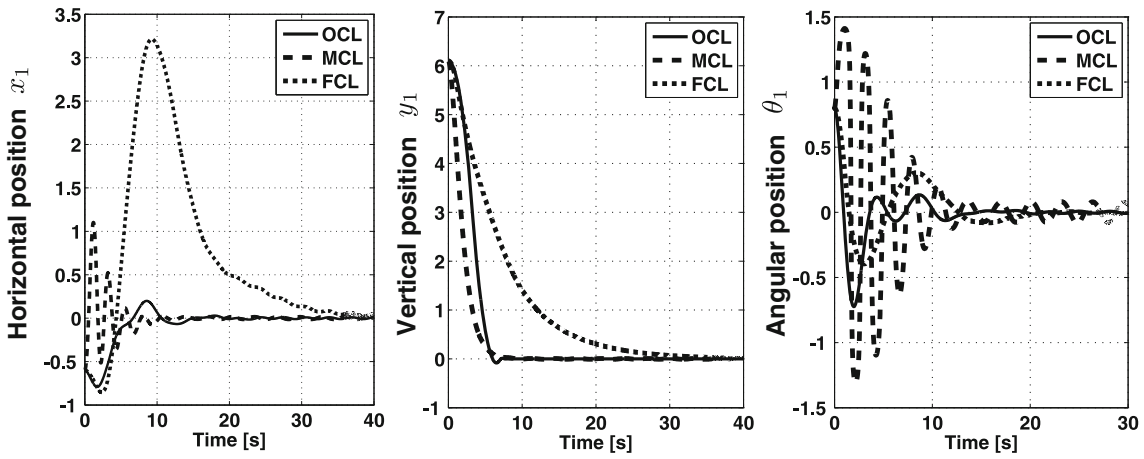

Fig. 2 Comparison of the closed-loop responses among **OCL**, **FCL**, and **MCL** for a hovering task and in presence of sustained small perturbations

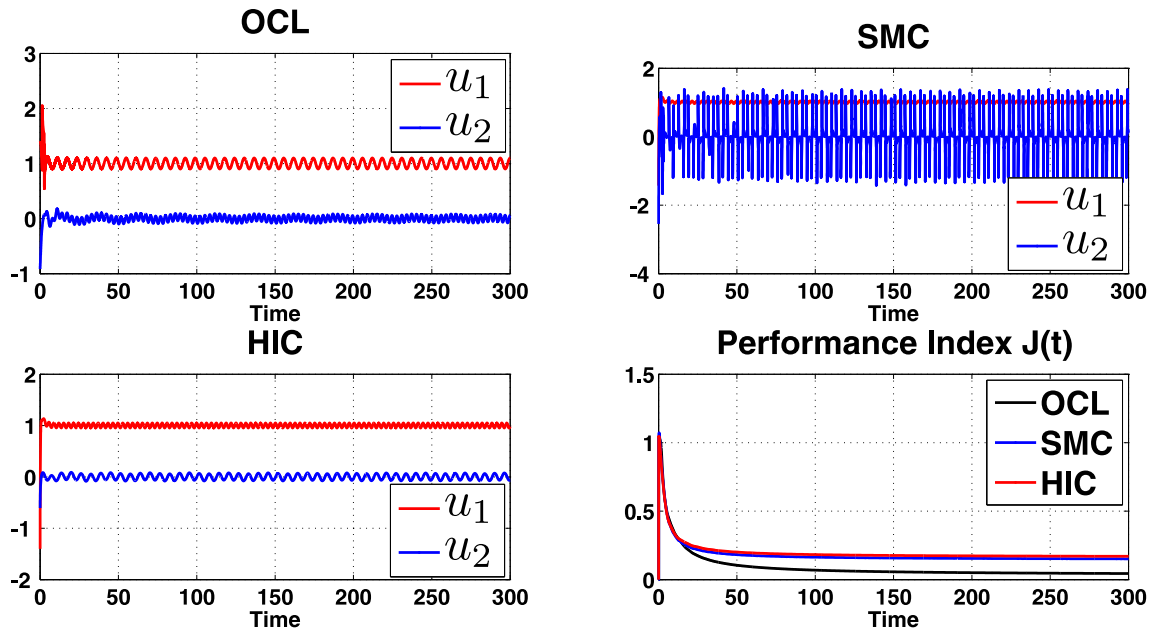

Fig. 3 Comparison of the closed-loop responses, in the presence of parametric uncertainties, among **OCL**, **SMC**, and **HIC** , for a regulation task from the initial condition, $q(0) = (y_1(0) = 1, x_1(0) = -0.2, \theta_1(0) = 0.2)$ and $\dot{q}(0) = 0$, to a neighborhood of the position zero, with $\epsilon = 0.1$

where:

$$\widehat{r} = s_r \left[L \left(\widetilde{y}_1 + \frac{\widehat{y}_2 |\widehat{y}_2|}{2r} \right) \right]; \quad \widehat{p} = (\widehat{x}_2, \widehat{y}_2, \widehat{\theta}_2).$$

Here, $\widehat{p}$ was generated using the following STBO algorithm:[3]

$$\begin{aligned} \dot{\widehat{q}} &= \widehat{p} - R_a \Phi \left[\widehat{q} - q \right]; \\ \dot{\widehat{p}} &= G(q, \widehat{p}) + R_3 \widehat{u}_2(q, \widehat{p}) - R_b \text{sgn} \left[\widehat{q} - q \right], \end{aligned} \tag{17}$$

where:

$$G(q, \widehat{p}) = \begin{bmatrix} \tan(\theta_1)(\widehat{r} - 1) \\ -\widehat{r} \\ 0 \end{bmatrix}; \; R_3 = \begin{bmatrix} 0 \\ 0 \\ 1 \end{bmatrix}, \tag{18}$$

and:

$$\Phi(\widehat{q} - q) = \left[\phi \left(\widehat{x}_1 - x_1 \right) \; \phi \left(\widehat{y}_1 - y_1 \right) \; \phi \left(\widehat{\theta}_1 - \theta_1 \right) \right],$$

with $\phi(x) = \text{sgn}[x] |x|^{\frac{1}{2}}$, and the gain matrices $R_a = diag(r_{a_1}, r_{a_2}, r_{a_3})$ and $R_b = diag(r_{b_1}, r_{b_2}, r_{b_3})$, with r_{a_i} and r_{b_i} being positive gains, chosen as follows:

$$\begin{aligned} &r_{a_i} > \epsilon; \quad r_{b_i} > \frac{(1+\zeta)(r_{a_i} + \epsilon)}{(1-\zeta)} \sqrt{\frac{2}{(r_{a_i} - \epsilon)}}; \\ &0 < \zeta < 1; \qquad\qquad i = \{1, 2, 3\}. \end{aligned} \tag{19}$$

Here, $\epsilon > 0$ is sufficiently large to reduce the time of convergence. Then, there exits some region around the equilibrium $\Phi \in \mathbb{R}^6$ that contains the equilibrium point $(q = \overline{q}, p = 0, \widehat{p} = 0)$, such that all the trajectories of system (1), in closed-loop with Eqs. 16 and 17, that start in Φ are bounded and satisfy:

$$\lim_{t \to \infty} (q(t), p(t), \widehat{p}(t)) = (\overline{q}, 0, 0).$$

[3] Similarly, $\widehat{q} = (\widehat{y}_1, \widehat{x}_1, \widehat{\theta}_1, \widehat{\theta}_2)$ is the estimation of variable q.

Proof Substituting the values of $\widehat{u}_1$ and $\widehat{u}_2$, given in Eq. 16, into system (1) leads to:

$$\begin{aligned} \dot{q} &= p; \\ \dot{p} &= G(q, \widehat{p}) + R_3 \widehat{u}_2(q, \widehat{p}). \end{aligned} \tag{20}$$

Defining the observation errors as $e_1 = \widehat{q} - q$ and $e_2 = \widehat{p} - p$, it is easy to see, from systems (20) and (18), that the error equations take the following form:

$$\begin{aligned} \dot{e}_1 &= e_2 - R_a \Phi \left[e_1 \right]; \\ \dot{e}_2 &= -R_b \text{sgn} \left[e_1 \right]. \end{aligned} \tag{21}$$

The proof of the finite time of convergence to zero of variables e_1 and e_2 is taken from the work of [12]. That is, it is assumed that $R_a > 0$ and $R_b > 0$ satisfy the inequalities given in Eq. 19. Then, observer (17) assures finite time convergence of the estimated states $(\widehat{q}, \widehat{p})$ to the actual states $(q, p) \in \mathbb{R}^3$. □

Convergence stability analysis sketch First of all, the following equality is fulfilled:

$$\widehat{p} = p + e_2 = (y_2 + e_{2(1)}, x_2 + e_{2(2)}, \theta_2 + e_{2(3)})^T, \tag{22}$$

where $e_{2(i)}$ is a bounded function with finite time of convergence to zero. Therefore, from the first and fourth equations of Eq. 20, we obtain[4]:

$$\begin{aligned} \dot{\widetilde{y}}_1 &= y_2; \\ \dot{y}_2 &= -s_r \left[L \left(\widetilde{y}_1 + \frac{\left(y_2 + e_{2(1)} \right) \left| y_2 + e_{2(1)} \right|}{2r} \right) \right]. \end{aligned}$$

[4] Remember that system (20) consists of six equations, because $q \in \mathbb{R}^3$ and $p \in \mathbb{R}^3$.

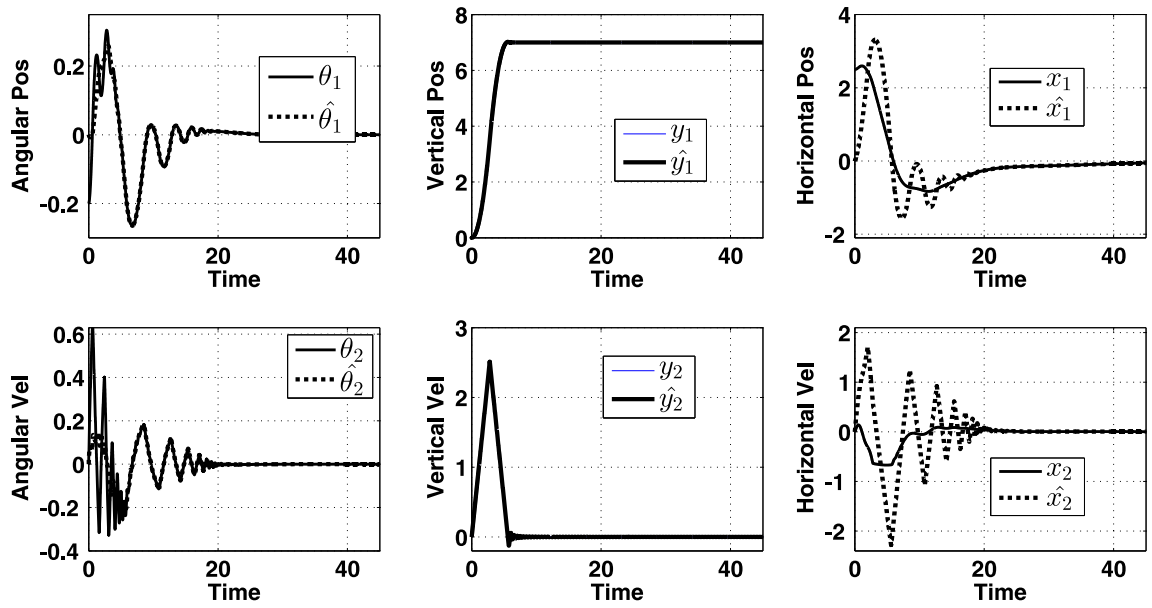

Fig. 4 Output-feedback responses of the PVTOL system for a hovering maneuver task. The initial and final positions were, respectively, $q_0 = (y_{1_0} = 0, x_{1_0} = 2.5, \theta_{1_0} = -0.2)$ and $q_\infty = (y_{1_\infty} = 7, x_{1_\infty} = 0, \theta_{1_\infty} = 0.0)$

Mimicking the ideas in **Lemma 1**, it can be concluded that the later system is **GAS**, because $e_{2(1)} \to 0$ in finite time. Besides, the last system does not show finite time of escape, because it is locally Lipschitz.

The remainder variables are analyzed using the system (4) in closed-loop with the second equation of Eq. 16. This closed-loop can be rewritten as:

$$\begin{aligned} \dot{z}_1 &= z_2; \\ \dot{z}_2 &= h[z_1, z_2] - b_2\lambda(m_3 e_{2(3)} + m_2 e_{2(2)}), \end{aligned} \tag{23}$$

where $b_2 = [0, 1]$, and $h[z_1, z_2]$ was proposed, such that:

$$\left[\frac{\partial V_T}{\partial Z}\right]^T \begin{bmatrix} z_2 \\ h[z_1, z_2] \end{bmatrix} = -\lambda(m_3\theta_2 + m_2 x_2)^2,$$

where the signals $e_{2(3)}$ and $e_{2(2)}$ asymptotically converge to zero in finite time. The invocation of well-known results from asymptotic stability of cascaded systems [41] completes the proof of local asymptotic stability. Consequently, it can be assured that z_1 and z_2 locally asymptotically converge to zero. Finally, it is shown that the trajectories of system (23) do not escape to infinity. From this, it is easy to

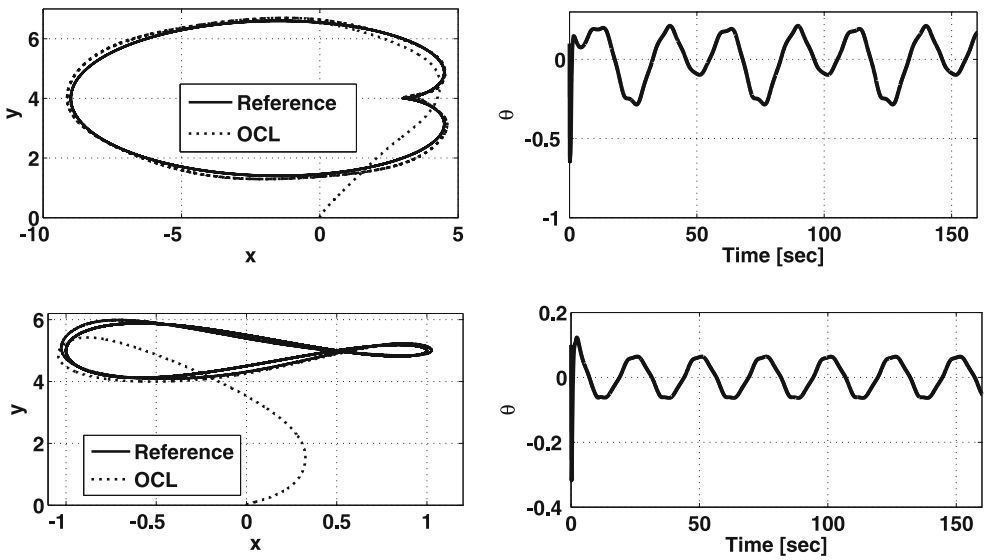

Fig. 5 Output-feedback trajectory tracking for two closed trajectories: a cardioid ($q_{\infty E}$) and an irregular lemniscate

see that the time derivative of V_T, around the trajectories of Eq. 23, leads to:

$$\dot{V}_T \leq \frac{1}{2}(m_3 e_{2_3} + m_2 e_{2_2})^2.$$

From the last inequality, it can be concluded that Z cannot exhibit finite time of escape, because $e_2 \to 0$ as long as $t \to t_*$. Evidently, after $t > t_*$, the function $\dot{V}_T$ becomes semi-definite negative.

Numerical simulations The performance of the proposed output-feedback control scheme was tested numerically, using two simulations. The first consisted of a hovering maneuver from the rest position:

$$q_0 = (y_{1_0} = 0, x_{1_0} = 2.5, \theta_{1_0} = -0.2),$$

to the final position:

$$q_\infty = (y_{1_\infty} = 7, x_{1_\infty} = 0, \theta_{1_\infty} = 0.0).$$

The numerical experiment used the same control gains as in Eq. 13, while the initial conditions of the **STBO** algorithm were set at the origin, and their gains were fixed as:

$$r_{a_1} = 2 \; r_{a_2} = 5 \; r_{a_3} = 2 \; r_{b_1} = 8.6 \; r_{b_2} = 12.2 \; r_{b_3} = 8.6\,.$$

The obtained results can be seen in Fig. 4, which shows that the evolution of the displacement in the space effectively moves the system from the initial position, q_0, to the final rest position, q_∞. The finite-time convergence of the estimated velocity, $\widehat{p}$, to the actual p can be realized after 16 seconds elapse. In addition, it can be noted that all variables are very close to the desired final rest position, after 50 seconds elapsed, the horizontal position having the worst convergence time, while the vertical position reaches its final position close to 5 seconds.

The second numerical experiment consisted of making the system follow two reference trajectories. The references were a cardioid ($q_{\infty E}$) and an irregular lemniscate ($q_{\infty L}$), respectively defined as:

$$q_{\infty E} = \Big(y_{1\infty_C} = 4 + (2\sin(\frac{t}{8}) - \sin(\frac{t}{4})), x_{1\infty_C} = 3(2\cos(\frac{t}{8}) - \cos(\frac{t}{4})), \theta_1 = 0\Big)$$

and

$$q_{\infty L} = \Big(y_{1\infty_L} = 5 - (\cos(\frac{3t}{8})\sin(\frac{t}{8})), x_{1\infty_L} = \cos(\frac{t}{4})), \theta_1 = 0\Big)$$

The control gains for the cardioid were selected as:

$$\begin{array}{lll} m_1 = 2.5 & m_2 = -\frac{1}{2} & m_3 = 2.5 \\ r = 2 & L = 220 & k_p = 2.6 \end{array},$$

and, for the irregular lemniscate, were selected as:

$$\begin{array}{lll} m_1 = 4.8 & m_2 = -1.5 & m_3 = 4.8 \\ r = 5 & L = 230 & k_p = 4.8 \end{array}.$$

In both cases, the initial conditions were fixed at the origin. The obtained results are shown in Fig. 5. From this figure, it can be seen that, even when our control strategy was designed for a different end, it was able to satisfactorily track both references.

5 Conclusion

An output-feedback control strategy for the regulation of a PVTOL aircraft is presented here. To this end, two controllers, that work simultaneously, were designed, assuming that the whole state is available. The first controller is devoted to stabilizing the vertical variable and is based on a simple feedback-linearization procedure in combination with a nonlinear controller that behaves like a terminal slide mode. The second controller, designed using an energy-control method, stabilizes the horizontal and angular variables to the desired rest position. Having proposed both controllers, a second-order sliding-mode observer for the exact velocities estimation was used. The proposed control strategy can be designed independently, due to the fact that the observer estimates the velocities in finite time. The closed-loop system was tested and illustrated through some numerical simulations, and comparisons with other control strategies.

Acknowledgments This research was supported by the Secretaría de Investigación y Posgrado of the Instituto Politecnico Nacional (SIP-IPN) under Research Grants 20171586 and 20171948.

Appendix

Proof of Lemma 1 Use the following Lyapunov function:

$$E(\alpha, \beta) = \int_0^{\alpha + \frac{\beta|\beta|}{2r}} s_r\,[Ls]\,ds + \frac{r\beta^2}{2},$$

whose time derivative, around the trajectories of Eq. 2, leads to:

$$\dot{E}(x, y) = -\frac{|\beta|}{r} s_r \left[L\left(\alpha + \frac{\beta\,|\beta|}{2r}\right)\right]^2.$$

which implies that $\dot{E}(\alpha, \beta) \leq 0$. As E is a strictly positive and non-increasing function, and α and β are bounded. Now, from LaSalle's invariance principle, as given in [25], all solutions of system (2) converge to the largest invariant set Θ, in $\left\{(\alpha, \beta) \in \mathbb{R}^2 : \dot{E}(\alpha, \beta) = 0\right\} = \{\beta = 0\} \cup \{\alpha + \frac{\beta|\beta|}{2r} = 0\}$. Computing the largest invariant set, it is easy to see that $\Theta = \{\alpha = \beta = 0\}$. Therefore, from LaSalle's

invariance, we conclude that all solutions of system (2) converge toward the invariant set $\Theta = \{0\}$. □

Comment 5 *Notice that the proposed E is radially bounded, as pointed out in* [43] *and* [35]. *That is,* $E \to \infty$ *as long as* $(\alpha, \beta) \to \infty$.

Design of the H_∞ -based linear controller First of all, we introduce the feedback $u_1 = 1 + v_1$. Then, we linearized, around the equilibrium point $(y_1 = \overline{y}_1, x_1 = \overline{x}_1, \theta_1 = \overline{\theta}_1)$, with $\varepsilon = 0$, the system (14). The obtained linearized system was expressed using the following decoupled pair of systems:

$$\begin{aligned} \dot{y} &= A_1 y + B_1 v_1 + B_1 \omega_1; \\ s_y &= C_1 y + v_1, \end{aligned} \tag{24}$$

and,

$$\begin{aligned} \dot{Z} &= A_2 Z + B_2 u_2 + B_3 \omega_{23}; \\ s_Z &= C_2 Z + u_2, \end{aligned} \tag{25}$$

where $y = (y_1, \dot{y}_1 = y_2)$, $Z = (x_1, \dot{x}_1 = x_2, \theta_1, \dot{\theta}_1 = \theta_2)$, and $\omega_{23}^T = [\omega_2, \omega_3]$ and:

$$A_1 = \begin{bmatrix} 0 & 1 \\ 0 & 0 \end{bmatrix};\ B_1 = \begin{bmatrix} 0 \\ 1 \end{bmatrix};\ C_1^T = \begin{bmatrix} 1 \\ 0 \end{bmatrix}$$

and:

$$A_2 = \begin{bmatrix} 0 & 1 & 0 & 0 \\ 0 & 0 & -1 & 0 \\ 0 & 0 & 0 & 1 \\ 0 & 0 & 0 & 0 \end{bmatrix};\ B_2 = \begin{bmatrix} 0 \\ 0 \\ 0 \\ 1 \end{bmatrix};\ B_3 = \begin{bmatrix} 0 \\ 1 \\ 0 \\ 1 \end{bmatrix};\ C_1^T = \begin{bmatrix} 1 \\ 1 \\ 0 \\ 0 \end{bmatrix}$$

Please notice that (s_y, s_z) are the penalty signals. In our case, the H_∞-control problem consisted of finding two controllers, v_1 and u_2, such that they stabilize, respectively, the systems (24) and (25), satisfying the following inequalities:

$$\begin{aligned} \int_{t_0}^{T} s_y^2(\tau) d\tau \ \le\ \gamma_1 \int_{t_0}^{T} \omega_1^2(\tau) d\tau;\ \int_{t_0}^{T} s_Z^2(\tau) d\tau \\ \le \gamma_{23} \int_{t_0}^{T} \|\omega_{23}(\tau)\|\, d\tau, \end{aligned}$$

where $\left\|T_{s_y \omega_1}\right\|_\infty < \gamma_1$, $\left\|T_{s_Z \omega_{23}}\right\|_\infty < \gamma_{23}$[5] and $v_1 = \overline{K}_1^T y$ and $u_2 = \overline{K}_2^T Z$ were obtained for the systems (24) and (25), respectively, solving some version of the Riccati equation [5]. Using the Matlab package we found that $\overline{K}_1$ and $\overline{K}_2$ coincided with Eq. 15, with $\gamma_1 = 1.1$ and $\gamma_{23} = 1.4$.

[5] T_{sw} denotes the transference function from w to z.

References

1. Acosta, J.A., Ortega, R., Astolfi, A., Mahindrakar, A.D.: Interconnection and damping assignment passivity-based control of mechanical systems with underactuation degree one. IEEE Trans. Autom. Control **50**(12), 1936–1955 (2005)
2. Benosman, M., Liao, F., Lum, K.Y.: Output trajectory tracking for the pvtol aircraft through control allocation. In: 2007. CCA 2007. IEEE International Conference on Control Applications, pp. 880–885. IEEE (2007)
3. Borrelli, F., Bemporad, A., Morari, M.: Predictive control for linear and hybrid systems. Camb. February **20**, 2011 (2011)
4. Cárdenas, R., Aguilar, L.T.: Output feedback sliding mode control of a pvtol including actuators dynamics. In: Control Applications (CCA), 2011 IEEE International Conference on, pp. 1482–1486. IEEE (2011)
5. Castaños, F., Fridman, L.: Analysis and design of integral sliding manifolds for systems with unmatched perturbations. IEEE Trans. Autom. Control **51**(5), 853–858 (2006)
6. Cerven, W.T., Bullo, F.: Constructive controllability algorithms for motion planning and optimization. IEEE Trans. Autom. Control **48**(4), 575–589 (2003)
7. Chemori, A., Marchand, N.: Global discrete-time stabilization of the pvtol aircraft based on fast predictive control. In: Proceedings of the 17th World Congress The International Federation of Automatic Control (2008)
8. Consolini, L., Maggiore, M., Nielsen, C., Tosques, M.: Path following for the pvtol aircraft. Automatica **46**(8), 1284–1296 (2010)
9. Corona-Sánchez, J.J., Rodríguez-Cortés, H.: Experimental real-time validation of an attitude nonlinear controller for the quadrotor vehicle. In: Unmanned Aircraft Systems (ICUAS), 2013 International Conference on, pp. 453–460. IEEE (2013)
10. Corona-Sánchez, J.J., Rodríguez-Cortés, H.: Trajectory tracking control for a rotary wing vehicle powered by four rotors. J. Intell. Robot. Syst. **70**(1-4), 39–50 (2013)
11. Davila, J.: Exact tracking using backstepping control design and high-order sliding modes. IEEE Trans. Autom. control **58**(8), 2077–2081 (2013)
12. Davila, J., Fridman, L., Levant, A.: Second-order sliding-mode observer for mechanical systems. IEEE Trans. Autom. Control **50**(11), 1785–1789 (2005)
13. Fantoni, I., Lozano, R.: Non-linear control for underactuated mechanical systems. Springer Science & Business Media, Berlin (2001)
14. Fantoni, I., Lozano, R., Castillo, P.: A simple stabilization algorithm for the pvtol aircraft. In: 15th IFAC World Congress (2002)
15. Fantoni, I., Palomino, A., Castillo, P., Lozano, R., Pégard, C.: Control strategy using vision for the stabilization of an experimental pvtol aircraft setup. In: Current Trends in Nonlinear Systems and Control, pp. 407–419. Springer (2006)
16. Frye, M.T., Ding, S., Qian, C., Li, S.: Global finite-time stabilization of a pvtol aircraft by output feedback. In: CDC/CCC 2009. Proceedings of the 48th IEEE Conference on Decision and Control, 2009 held jointly with the 2009 28th Chinese Control Conference, pp. 2831–2836. IEEE (2009)
17. Gandolfo, D., Rosales, C., Patiño, D., Scaglia, G., Jordan, M.: Trajectory tracking control of a pvtol aircraft based on linear algebra theory. Asian J. Control **16**(6), 1849–1858 (2014)
18. Garcia, P.C., Lozano, R., Dzul, A.E.: Modelling and control of mini-flying machines. Springer Science & Business Media, Berlin (2006)
19. Gruszka, A., Malisoff, M., Mazenc, F.: On tracking for the pvtol model with bounded feedbacks. In: American Control Conference (ACC) 2011, pp. 1428–1433. IEEE (2011)

20. Guadarrama-Olvera, J.R., Corona-Sánchez, J.J., Rodríguez-Cortés, H.: Hard real-time implementation of a nonlinear controller for the quadrotor helicopter. J. Intell. Robot. Syst. **73**(1-4), 81–97 (2014)
21. Gupta, A., Mejari, M., Ketkar, V., Datar, M., Singh, N.M.: Nonlinear model predictive control of pvtol aircraft under state and input constraints. In: Proceedings of Conference on Advances In Robotics, pp. 1–6. ACM (2013)
22. Han, J.: From pid to active disturbance rejection control. IEEE Trans. Ind. Electron. **56**(3), 900–906 (2009)
23. Hauser, J., Sastry, S., Meyer, G.: Nonlinear control design for slightly non-minimum phase systems: application to v/stol aircraft. Automatica **28**(4), 665–679 (1992)
24. Huang, C.S., Yuan, K.: Output tracking of a non-linear non-minimum phase pvtol aircraft based on non-linear state feedback control. Int. J. Control **75**(6), 466–473 (2002)
25. Khalil, H.K., Grizzle, J.: Nonlinear systems, vol. 3. Prentice Hall, Upper Saddle River (2002)
26. Lin, F., Zhang, W., Brandt, R.D.: Robust hovering control of a pvtol aircraft. IEEE Trans. Control Syst. Technol. **7**(3), 343–351 (1999)
27. Lozano, R., Castillo, P., Dzul, A.: Global stabilization of the pvtol: real-time application to a mini-aircraft. Int. J. Control **77**(8), 735–740 (2004)
28. Lu, X.Y., Spurgeon, S.K., Postxethwaite, I.: Robust variable structure control of a pvtol aircraft. Int. J. Syst. Sci. **28**(6), 547–558 (1997)
29. Maqsood, A., Go, T.H.: Multiple time scale analysis of aircraft longitudinal dynamics with aerodynamic vectoring. Nonlinear Dyn. **69**(3), 731–742 (2012)
30. Marconi, L., Isidori, A., Serrani, A.: Autonomous vertical landing on an oscillating platform: an internal-model based approach. Automatica **38**(1), 21–32 (2002)
31. Martin, P., Devasia, S., Paden, B.: A different look at output tracking: control of a vtol aircraft. In: 1994., Proceedings of the 33rd IEEE Conference on Decision and Control, vol. 3, pp. 2376–2381. IEEE (1994)
32. Munoz, L.E., Santos, O., Castillo, P.: Robust nonlinear real-time control strategy to stabilize a pvtol aircraft in crosswind. In: 2010 IEEE/RSJ International Conference on Intelligent Robots and Systems (IROS), pp. 1606–1611. IEEE (2010)
33. Nielsen, C., Consolini, L., Maggiore, M., Tosques, M.: Path following for the pvtol: A set stabilization approach. In: 2008. CDC 2008. 47th IEEE Conference on Decision and Control, pp. 584–589. IEEE (2008)
34. Notarstefano, G., Hauser, J., Frezza, R.: Trajectory manifold exploration for the pvtol aircraft. In: CDC-ECC'05. 44th IEEE Conference on Decision and Control, 2005 and 2005 European Control Conference, pp. 5848–5853. IEEE (2005)
35. Olfati-Saber, R.: Global configuration stabilization for the vtol aircraft with strong input coupling. IEEE Trans. Autom. Control **47**(11), 1949–1952 (2002)
36. Ortega, R., Garcia-Canseco, E.: Interconnection and damping assignment passivity-based control: A survey. Eur. J. control **10**(5), 432–450 (2004)
37. Palomino, A., Castilto, P., Fantoni, I., Lozano, R., Pégard, C.: Control strategy using vision for the stabilization of an experimental pvtol aircraft setup. IEEE Trans. Control Syst. Technol. **13**(5), 847–850 (2005)
38. Qiu, H., Duan, H.: Receding horizon control for multiple uav formation flight based on modified brain storm optimization. Nonlinear Dyn. **78**(3), 1973–1988 (2014)
39. Rubio, J.d.J., Cruz, J.P., Zamudio, Z., Salinas, A.: Comparison of two quadrotor dynamic models. IEEE Latin Amer. Trans. **12**(4), 531–537 (2014)
40. Sastry, S.: Nonlinear systems: analysis, stability, and control, vol. 10. Springer, New York (1999)
41. Sepulchre, R., Jankovic, M., Kokotovic, P.: Constructive nonlinear control. Springer, Berlin (1997)
42. Sira-Ramirez, H., Fliess, M.: Regulation of non-minimum phase outputs in a pvtol aircraft. In: 1998. Proceedings of the 37th IEEE Conference on Decision and Control, vol. 4, pp. 4222–4227. IEEE (1998)
43. Teel, A.R.: A nonlinear small gain theorem for the analysis of control systems with saturation. IEEE Trans. Autom. Control **41**(9), 1256–1270 (1996)
44. Turker, T., Oflaz, T., Gorgun, H., Cansever, G.: A stabilizing controller for pvtol aircraft. In: 2012 American Control Conference (ACC), pp. 909–913. IEEE (2012)
45. Venkatesh, C., Mehra, R., Kazi, F., Singh, N.: Passivity based controller for underactuated pvtol system. In: 2013 IEEE International Conference on Electronics, Computing and Communication Technologies (CONECCT), vol. 1–5. IEEE (2013)
46. Wood, R., Cazzolato, B.: An alternative nonlinear control law for the global stabilization of the pvtol vehicle. IEEE Trans. Autom. Control **52**(7), 1282–1287 (2007)
47. Wood, R., Cazzolato, B., Halim, D.: A global non-linear control design for a pvtol vehicle with aerodynamics. In: 2005 and 2005 European Control Conference. CDC-ECC'05. 44th IEEE Conference on Decision and Control, pp. 7478–7483. IEEE (2005)
48. Xian, B., Diao, C., Zhao, B., Zhang, Y.: Nonlinear robust output feedback tracking control of a quadrotor UAV using quaternion representation. Nonlinear Dynamics **79**(4), 2735–2752 (2015)
49. Zavala-Río, A., Fantoni, I., Lozano, R.: Global stabilization of a pvtol aircraft model with bounded inputs. Int. J. Control **76**(18), 1833–1844 (2003)
50. Zhu, B., Wang, Q., Huo, W.: Longitudinal–lateral velocity control design and implementation for a model-scaled unmanned helicopter. Nonlinear Dyn. **76**(2), 1579–1589 (2014)

Carlos Aguilar-Ibañez was born in Tuxpan, Veracruz, Mexico. He graduated in Physics at the Higher School of Physics and Mathematics of the National Polytechnic Institute (IPN), Mexico City 1990. From the Research Center and Advanced Studies of the IPN (Cinvestav-IPN) he received the M.S. degree in Electrical Engineering in 1994, and a Ph.D. in Automatic Control in 1999. Ever since he has been a researcher at the Center of Computing Research of the IPN (CIC-IPN). As of 2000 he belongs to the National System of Researchers (SNI) of Mexico. His research focuses in nonlinear systems, system identification, observers, automatic control, and chaos theory.

Miguel S. Suarez-Castanon was born in Mexico City, Mexico, in 1967. He received a B.S. degree in Cybernetics and Computer Science from the School of Engineering of the Lasalle University in 1989. From the Research Institute of Applied Mathematics and Systems he received the M.S. degree in Computer Sciences in 2001. In 2005 he received a Ph.D. in Computer Sciences from the CIC-IPN. Since 2007 he is a member of the SNI of Mexico.

Julio Mendoza-Mendoza concluded his computing doctoral degree at CIC IPN in 2016, where he specialised in underactuated robotics, UAS, and intelligent and nonlinear control. Also he achieved his advanced technologies master degree and mechatronics-engineering bachelor at UPIITA IPN, in 2011 and 2008 respectively. Since that time he developed his interest areas and research in robot manipulators, mobile robots, humanoids, underactuated systems, UAVs, and various control techniques. Nowadays he works in 2 patents related with his research field and develops the flying serial-robot manipulator theory.

Jose de Jesus Rubio is a full time professor of the Sección de Estudios de Posgrado e Investigación, ESIME Azcapotzalco, Instituto Politécnico Nacional. He has published 101 papers in International Journals, 1 International Book, 8 chapters in International Books, and 31 papers in International Conferences with 630 citations. He is a member of the IEEE AFS Adaptive Fuzzy Systems. He is member of the National Systems of Researchers with level II. He has been the tutor of 4 post Ph.D. student, 8 Ph.D. students, 32 M.S. students, 4 S. students, and 17 B.S. students.

Juan Carlos Martínez-García was born in Tlalnepantla, Mexico, in 1964. He received the Diploma in mechanical and electrical engineering from the National Autonomous University of Mexico and the M.Sc. degree in electrical engineering from the Center for Advanced Studies and Research of the National Polytechnic Institute of Mexico (Cinvestav-IPN), in 1989 and 1991, respectively. He received the Ph.D. degree (Summa Cum Laude) in mathematical control theory from Ecole Centrale Nantes, Nantes, France, in 1994. He is Professor on Control Theory at Cinvestav-IPN. His current research interests include robustness analysis of linear and nonlinear systems, evolutionary robotics (as a mean to elucidate natural evolutionary phenomena), fault diagnosis in dynamical systems, and applications of feedback control and identification in several disciplines including earthquake engineering, nonlinear mechanical systems and systems biology (mainly network-based structural properties involved in biological functionalities). He is concerned by the interplay between art and science, understood in terms of regulatory dynamics.